First principles study of the optical emission of cadmium yellow: Role of cadmium vacancies

Laura Giacopetti,[1,2,a] Austin Nevin,[3,b] Daniela Comelli,[4,c] Gianluca Valentini,[4,d] Marco Buongiorno Nardelli,[5,e] and Alessandra Satta[1,f]

[1]*CNR-IOM Cagliari, c/o Dipartimento di Fisica, Università di Cagliari, Cittadella Universitaria, 09042 Monserrato, Italy*
[2]*Dipartimento di Scienze Chimiche e Geologiche, Università di Cagliari, Cittadella Universitaria, 09042 Monserrato, Italy*
[3]*CNR-IFN Milano, Piazza Leonardo da Vinci, 20133 Milano, Italy*
[4]*Dipartimento di Fisica, Politecnico di Milano, Piazza Leonardo da Vinci, 20133 Milano, Italy*
[5]*Department of Physics, University of North Texas, Denton, Texas 76203, USA*

We study the role of structural defects in the CdS-based cadmium yellow paint to explain the origin of its deep trap states optical emission. To this end, we combine a first principles study of Cd- and S- vacancies in the wurtzite ($10\bar{1}0$) CdS surface with experimental photoluminescence spectroscopy of the commercial hexagonal CdS pigment. Computational results clearly state that the presence of cadmium vacancies in the pigment surface alters the electronic structure of cadmium sulfide by forming acceptor levels in the gap of the semiconductor. Such levels are consistent with the optical emission from trap state levels detected in the CdS pigment. This finding provides a first step towards the understanding of the photo-physical mechanisms behind the degradation of this modern pigment, widely used in impressionist and modernist paintings. © 2018 Author(s). All article content, except where otherwise noted, is licensed under a Creative Commons Attribution (CC BY) license (*http://creativecommons.org/licenses/by/4.0/*). https://doi.org/10.1063/1.5018512

Metal-based semiconductors have been widely used as colour pigments in impressionist, post-impressionist and early modern works from the 1880s through the 1920s. In particular, the brilliant yellow pigment takes its colouration from cadmium sulfide (CdS), a II-VI wide-gap semiconducting compound. The strong yellow colouration appeared in the works of Vincent van Gogh followed by prominent artists such as Claude Monet, Pablo Picasso and Henry Matisse. It was early recognised that poor quality Cadmium yellow tended to loose its colour in light, and recommendations to insure the absence of free sulphur in cadmium yellows were made.[1] Various cadmium yellow pigments undergo an irreversible degradation process, causes of which are still unclear. Discolouration (fading and darkening), formation of crumbly surfaces and of whitish semitransparent globules have been reported. Recent microscopy and spectroscopy studies on Ensor, Matisse, and Van Gogh paints[2–6] have partially elucidated the chemistry behind discoloration mechanisms, with the identification and mapping of different photo-oxidation products in altered paint layers, cadmium carbonates, sulfates and oxalates. However, the trigger mechanism for this irreversible degradation is still unknown. It has been suggested that paint alteration could be ascribed to an initial photo-oxidation of CdS:[7] excitation of the material by visible light results in the formation of electron/hole pairs which, following surface migration, produce redox chemistry and organic oxidation. Cadmium sulfide is observed in many pigments in the hexagonal wurtzite phase[6,8] - that is confirmed to be the main crystalline constituent

[a]laura.giacopetti@dsf.unica.it
[b]austin.nevin@ifn.cnr.it
[c]daniela.comelli@polimi.it
[d]gianluca.valentini@polimi.it
[e]Marco.BuongiornoNardelli@unt.edu
[f]alessandra.satta@cnr.it; Corresponding author

of the yellow paint. Beyond the specific field of Cultural Heritage, the physical properties of CdS have been widely studied due to their importance in fundamental science as well as in optoelectronic applications like solar cells,[9,10] lasers,[11,12] and recently in nanotechnology.[13,14]

In this Letter, we study the role of structural defects in hexagonal CdS to explain the origin of its well-known optical emission from deep trap states. Indeed, these crystal defects could be the precursors of the CdS degradation process. Among native defects we focus on cation and anion vacancies since other types of intrinsic defects were shown to give a yield that is not compatible with a deep trap state.[15–17] In particular, we focus on the role of Cd- and S- vacancies in the most stable CdS surface, namely the {10.0}. Their influence on the electronic structure of cadmium sulfide is studied by means of a first principles method in combination with experimental photoluminescence (PL) spectroscopy measurements on the commercial undeteriorated hexagonal CdS pigment.

Photoluminescence emissions due to deep trap states are observed both in pure commercial[18–20] and historical degraded pigments[18,21] supporting the basic idea that traps are intrinsic to CdS. The identification of these trap states is an essential step to understand the chemical reactivity of the unaltered pigment and to provide a reliable starting point for future studies on the complex mechanisms involved in the deterioration of a CdS paint.

In the present work, PL spectroscopy has been performed on hexagonal CdS-based pigment by employing a compact spectrometer and UV-laser excitation. Details on the employed PL spectrometer and on analysis of experimental data are provided in the supplementary material. First principles calculations have been carried out within the density functional theory in the generalized gradient approximation (DFT-GGA) as implemented in the quantum-ESPRESSO[22] package, using ultrasoft-PBE pseudopotentials.[23,24] To improve the description of the electronic properties and to correct the band gap we used ACBN0, a novel pseudo-hybrid Hubbard density functional that was recently developed by some of us.[25] Additional details on the computational set up are given in the supplementary material.

The relaxed clean $(10\bar{1}0)$ CdS surface showed the typical ridged profile where both cations and anions occupy two non-equivalent lattice sites, namely *top* and *hollow* positions (see supplementary material). We will refer to V_{Cd}^{top}, V_{Cd}^{hollow} and to V_S^{top}, V_S^{hollow} to indicate cadmium and sulfur vacancies, respectively. We focused first on cadmium vacancies since they were shown in benchmark calculations[26–28] to play a key-role in the surface reactivity. As for V_{Cd}^{top}, the corresponding density of states (DOS) (top panel in Fig. 1c) shows that the defective surface and the clean one (shaded area) differ in the presence of two states in the band gap due to a residual of the spin-down contribution: a shallow level close to valence band edge and a deep one. The projected DOS (central panel) reveals that this defect states are two acceptor levels, two electron holes, originating from the $3p$-dangling bonds of sulfur nearest neighbours (S_{NN}) lying in-plane. No contribution is detected from $S_\perp$ atoms in the interior layers (bottom panel), as well as equally negligible are the contributions from $Cd_\perp$. Similarly, for V_{Cd}^{hollow} a double acceptor level appears on top of the valence band maximum. In Fig. 2c), top panel, the vacancy DOS (red curve) follows different spin up and down profiles and still, the acceptor state is a p-like spin-down residual due to S_{NN}. At variance with what is shown for V_{Cd}^{top}, the $S_\perp$ undergoes a remarkable upward relaxation where the $3p$-states (green line in the bottom panel of Fig. 2c) participate to the formation of the acceptor level. Interior sulfur atoms lying in the bulk region of the slab (violet line in the bottom panel) do not show any spin-asymmetry and no contribution to the extra level in the gap confirming that unpaired p electrons of sulfur atoms decorating the vacancy site are solely responsible for: *i*) the formation of trap states in the gap; *ii*) a localised ferromagnetic behaviour. In fact, the total magnetic moment calculated in the defective surface, $1.45\mu_B$ and $1.72\mu_B$ for *top* and *hollow* cadmium vacancies, respectively, results only from the contributions of S_{NN}. While the structural properties are reliably predicted in DFT-GGA, the electronic structure suffers the underestimation of the bandgap. To improve such a description the band structure and the DOS were also determined, in few relevant cases of the present study, by the use of the ACBN0 functional that was recently successfully applied, among others, to CdS bulk.[29] The calculated energy gap E_g^{ACBN0}=2.30 eV differs by 5% compared to the experimental one E_g^{exp}=2.42 eV with a remarkable improve of the the standard DFT-GGA value ($E_g^{DFT-GGA}$=1.19 eV). The recalculated band structure and the DOS are reported in Figure 3, where the deep trap electron state is confirmed to be located in the bandgap. It is interesting to note that there are several analogies with the isoelectronic ZnO {10.0} surface
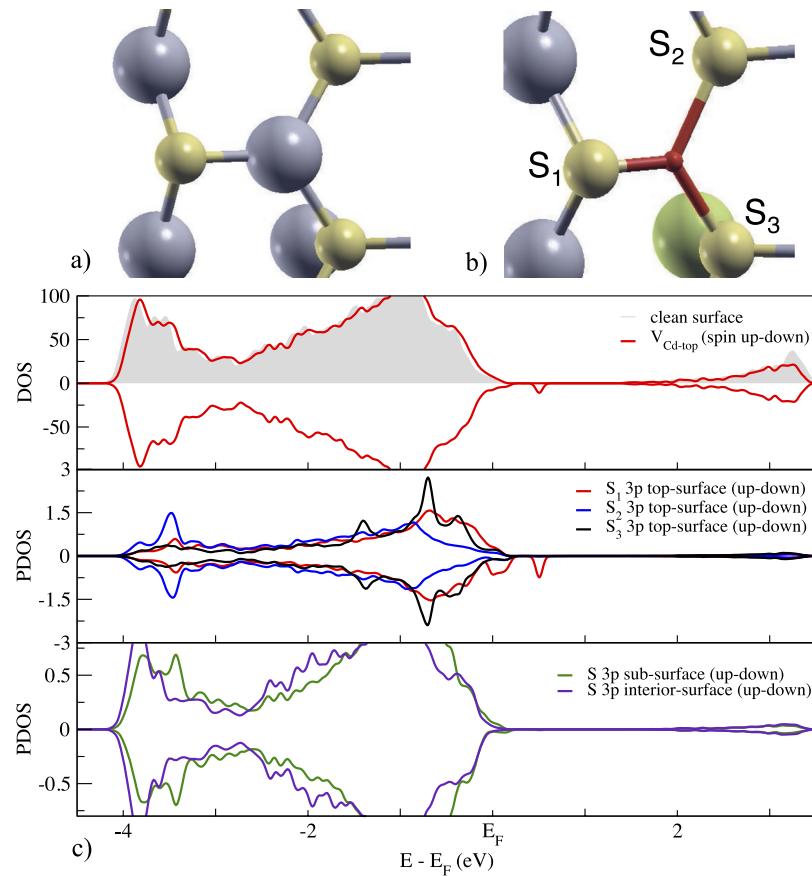
FIG. 1. V_{Cd}^{top}- Top-view of unrelaxed (a) and relaxed (b) geometry of the CdS {10.0} defective surface. In red, vacancy surrounding bonds. Total DOS of clean (shaded area) and defective surface, and PDOS of S-3p dangling bonds (c).

for which it was demonstrated[30] that the green luminescence is only assigned, in the presence of Zn vacancy, to the unpaired O p-electrons that give rise to empty states in the gap and to a residual spin magnetisation.

Sulfur vacancies both in *top* and *hollow* positions lead (see supplementary material) to a slight rearrangement of the band edges but no remarkable effects within the gap region. For this reason we will focus henceforth on cadmium vacancies.

The presence of electrically active defects may affect recombination rates and cause optical absorption or luminescence. As already mentioned, a considerable underestimation of semiconductor band gap is a shortcoming of the DFT approach.[31] The moderately large size of the defective surface considered makes the use of proper GW[32] and recent hybrid functionals[33] computationally prohibitive. To estimate the optical transitions we adopted an affordable method based on the formalism of formation energies, successfully applied in a variety of wide gap semiconductors and insulators[34] that required some *a posteriori* corrections[35] to remove long-ranged Coulomb interactions between charged-defects images due to the periodic boundary conditions. More specifically, we combined the formation energies of V_{Cd}^{top} and V_{Cd}^{hollow} defects in the neutral and negative charge states, namely $q = 0, -1, -2$. The vacancy formation energies, E_f, were calculated in both S-rich and Cd-rich growth conditions. Results are summarised in Table I where E_f for V_{Cd}^{bulk} calculated in a bulk containing up to 128 lattice sites is reported as reference. Formation energies for neutral surface vacancies are lower, as expected, than those calculated in the bulk. The value obtained with similar studies,[36] 2.26 eV for neutral Cd vacancies in hexagonal bulk under S-rich conditions, is in fair agreement with our model. Discrepancy is due to the different chemical potential adopted. In average, vacancy formation energies calculated under Cd-rich growth conditions (~3.59 eV) are higher than those in S-rich (~2.40 eV). Such values related to the non entropic part of the Gibbs free energy of formation
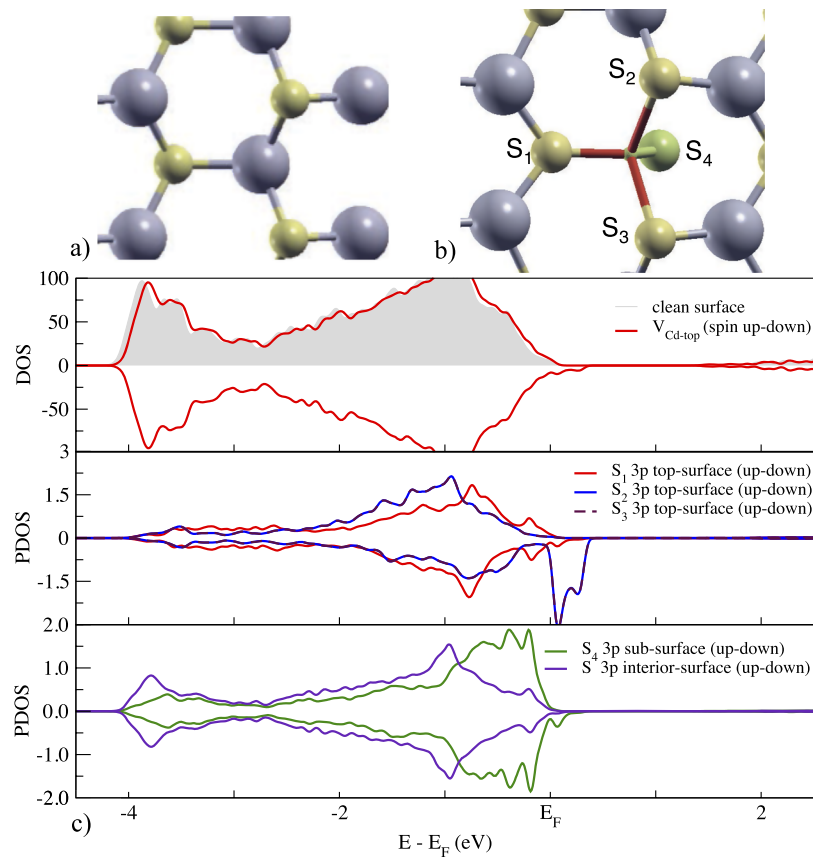
FIG. 2. V_{Cd}^{hollow} - Top-view of unrelaxed (a) and relaxed (b) geometry of the CdS {10.0} defective surface. In red, vacancy surrounding bonds. Total DOS of clean (shaded area) and defective surface, and PDOS of S-3p dangling bonds (c).

allow us to have an estimate of the concentration of vacancies per cm^3 (number of defects/number lattice sites) at thermal equilibrium through to the Law of Mass Action, *i.e.* $c_{eq} \propto e^{-E_f/k_B T}$. It turns out that at calcination temperature (~600°C) the ratio c_{eq}[S-rich] $\approx 10^9$ cm^{-3} vs. c_{eq}[Cd-rich] $\approx 10^2$ cm^{-3} emphasizes that yellow pigments grown under Cd-rich environmental conditions are more stable than those created under S-rich.

We found a deep acceptor level in PL measurements of the hexagonal CdS-based pigment: in experimental data, beside the narrow emission peak centered at 2.41 eV (see supplementary material) ascribed to radiative emission via near-band edge recombination, we have detected a broad near-infrared asymmetric emission (generically centered around 1.57 eV), ascribed to the presence of multiple energy levels inducing optical transitions in the range 1.4 - 1.8 eV (Figure 4). The emission lifetime $\tau = 6.0$ μs (see supplementary material) confirms that this optical transition occurs from trap state levels. Also, part of an emission centered at energies lower than the ones achievable with the available detector (> 1.3 eV) is visible in Figure 4. The reported experimental results are in good agreement with the few research studies carried out on the near-infrared optical emission of cadmium-based pigments associated with trap states.[18–20] Rosi et al.,[20] following analysis of the commercial pigment based on hexagonal CdS, has reported two distinct trap state peaks at 1.24 eV and 1.64 eV. Interestingly, in the analytical-grade hexagonal CdS reference sample they detected only a single peak at 1.57 eV. Commenting on the observed difference, authors suggested that crystalline composition is not the only factor affecting the PL emission properties but the location of defects (bulk vs surface), the concentration, and the defect structure itself play a relevant role. In Cesaratto et al.[19] the kinetic emission properties of commercially available cadmium-based pigments has been first reported, with near-infrared optical transitions from trap state levels being characterized by emission lifetimes on the order of tens of microseconds uncorrelated with pigment chemical composition.
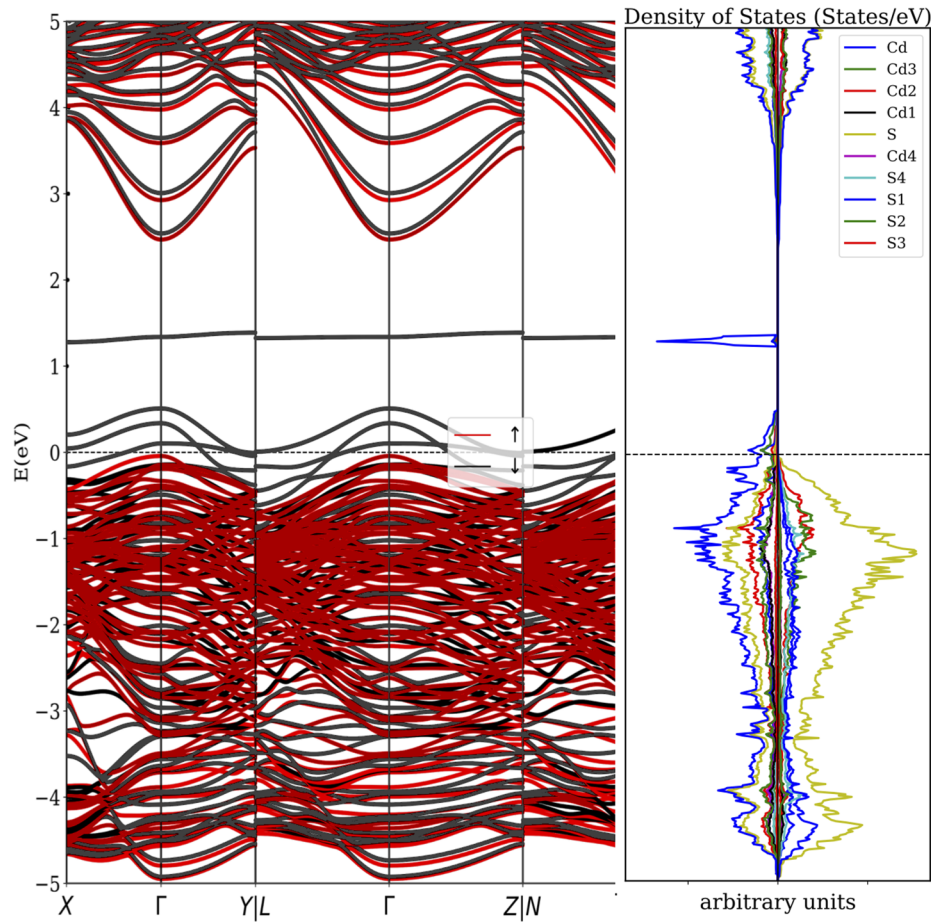
FIG. 3. ACBN0 for V_{Cd}^{top}: Band structure (left) and DOS (right) of defective surface. Red and black curves represent spin up and down electron states, respectively. Dotted line at E=0 represents the Fermi energy. Different colours in the DOS refer to different chemical elements around the vacancy.

The theoretical optical emission (luminescence) energy $\epsilon^{opt}(q/q')$ due to the recombination from the defect level into the valence band maximum (VBM) was calculated as a linear combination of the formation energies of the defect in different charge states as illustrated in Refs. 34 and 37. Also, spurious electrostatic interactions of charged defects due to the periodic boundary conditions were removed in the calculations of formation energies. The ACBN0 gap for CdS (E_g = 2.30 eV) is here assumed as the gap amplitude. Fig. 5 summarises $E_f[V_{Cd}]$, calculated for *top* and *hollow* Cd-vacancies under S-rich (shaded area) and Cd-rich conditions, versus the chemical potential of the electron reservoir denoted as the Fermi energy offset from VBM up to conduction band minimum CBM = E_g. The white vertical region encloses the experimental range (1.4 - 1.8 eV) of the broad measured PL emission detected in our sample.

TABLE I. Formation energies, E_f (eV), for surface *top* and *hollow* Cd vacancies both in neutral and negatively charged states, under S-rich and Cd-rich conditions. E_f computed in bulk CdS are also reported.

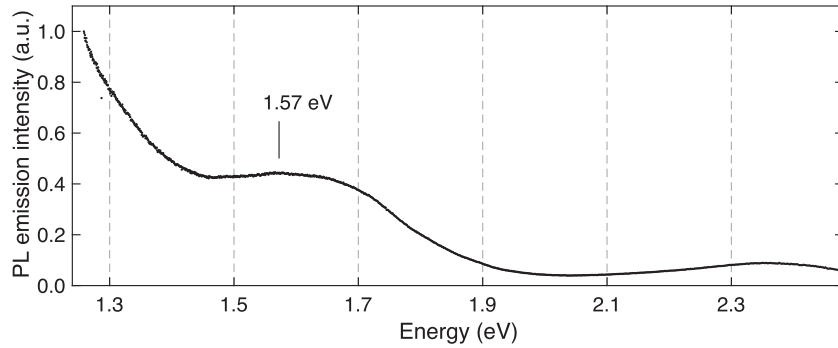|	V_{Cd}^{top}			V_{Cd}^{hollow}			V_{Cd}^{bulk}
q	0	-1	-2	0	-1	-2	0
S-rich	2.12	3.09	4.83	2.68	3.80	5.30	2.81
Cd-rich	3.31	4.29	6.02	3.87	4.99	6.48	4.12

FIG. 4. PL emission Spectrum of the hexagonal CdS pigment following continuous-wave excitation with a power density of 0.1 W/cm^2.

V_{Cd}^{top} under S-rich conditions appears as the most favoured defect inducing an optical transition state $\epsilon^{opt}(-1/-2)$=1.74 eV in excellent agreement with our experimental result. Also V_{Cd}^{hollow} shows the same kind of transition at 1.50 eV consistently with the measurements but at higher formation energies. Further, calculated optical transitions at 0.97 and 1.12 eV for *top* and *hollow*, respectively, attributed to transitions 0/− are consistent with the emission detected at energy < 1.3 eV. Under Cd-rich conditions we find the same behaviour with V_{Cd}^{top} favorite to V_{Cd}^{hollow} and still, the transition $(-1/-2)$ is the one compatible with the deep trap emission.

As for the sample of hexagonal CdS examined in this work, information on the process used for its synthesis is not accessible, but is likely to be based on the use of excess sulfuric acid to yield CdSO$_4$ which is then reacted with an alkali sulphide to precipitate CdS. Calcination of the precipitate converts cubic to hexagonal CdS.[38] Thus it is not clear, in general, if synthesis results in the formation of Cd or S vacancies, both of which are reported in literature for CdS-based materials.[38] In both cases,
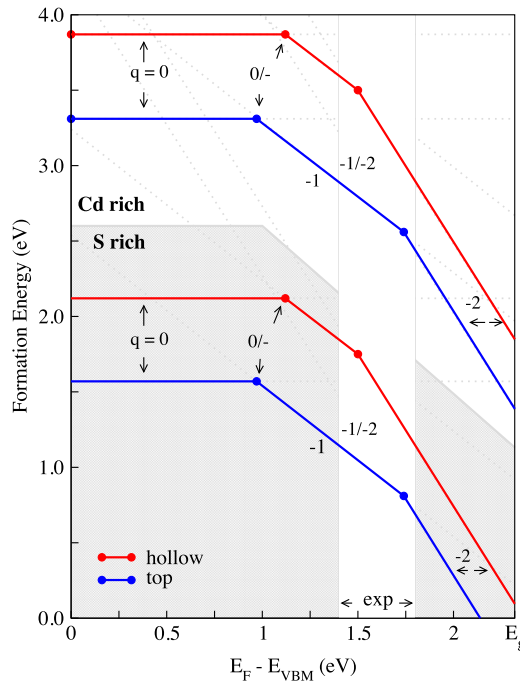

FIG. 5. E_f vs. Fermi energy for Cd vacancies in CdS surface under S-rich (shaded region) and Cd-rich simulated environmental growth conditions. Red and blue curves refer to *hollow* and *top* Cd vacancies, respectively. The zero of Fermi level corresponds to the valence band maximum. The slope of segments indicates the charge state. Kinks in the curves indicate transitions between different charge states.

assuming unintentionally doped sample as an n-type,[39] an excess of free electrons, i.e. donor states, would raise the Fermi level just below the CBM. We can propose two different scenarios:

i) *Cd-rich* - the n-type sample would contain an excess of S vacancies (and/or Cd interstitials). From our calculations, the formation energy for S vacancies is the lowest (highest concentration), both in the bulk and in the surface. The surface Cd vacancies show the highest formation energy (lowest concentration). Their presence in the surface can be ascribed to oxidation mechanisms occurring after the growth. We determined the formation energies of V_{Cd}^{top} considering different chemical potentials for Cd calculated from solid CdO and CdO_2. The values obtained, 1.23 and 1.63 eV, respectively, are significantly lower with respect to those reported in Table I. Similarly, considering cadmium chemical potential obtained from typical secondary compounds observed in historical deteriorated paints,[40] i.e. $CdCl_2$, $CdSO_4$, $CdCO_3$, E_f for V_{Cd}^{top} resulted in 0.21, 3.01 and 3.60 eV, respectively. Hence, we speculate that oxygen and chlorine present in the environment likely form Cd-based secondary compounds. $CdSO_4$ and $CdCO_3$, with higher formation energies, may support the hypothesis of residual starting reagents.

ii) *Cd-poor* (S-rich) - the n-type sample would have an excess of free electrons but the concentration of S vacancies at thermal equilibrium in the as-grown sample would be lower while the concentration of surface Cd vacancies would be higher (lower formation energy) than those in Cd-rich. Further oxidising reactions would increase the level of superficial damage.

In summary, we have combined a first principles study at different levels of theory on surface intrinsic defects with photoluminescence spectroscopy in hexagonal CdS in order to interpret the origin of a deep trap state often detected through photoluminescence both in commercial and historical deteriorated yellow pigments. Results clearly show, for the first time, that such emission represents an electron/hole recombination occurring in the presence of surface cadmium vacancies: the sulfur 3p dangling bonds created by the missing cation are the origin of the deep acceptor level in the gap experimentally observed.

See supplementary material for a complete description of both experimental and theoretical setups. Additional theoretical results on S vacancy and Cd and S self-interstitial are also reported.

[1] G. Buchner, *Über Schwefelcadmium und ber die verschiedenen Cadmiumfarben des Handels*, edited by G. Krause, Vol. 11 (1887) pp. 1087–1089.

[2] J. Mass, J. Sedlmair, C. S. Patterson, D. Carson, B. Buckley, and C. Hirschmugl, Analyst **138**, 6032 (2013).

[3] J. L. Mass, R. Opila, B. Buckley, M. Cotte, J. Church, and A. Mehta, Applied Physics A **111**, 59 (2013).

[4] G. Van der Snickt, J. Dik, M. Cotte, K. Janssens, J. Jaroszewicz, W. De Nolf, J. Groenewegen, and L. Van der Loeff, Analytical Chemistry **81**, 2600 (2009).

[5] E. Pouyet, M. Cotte, B. Fayard, M. Salomé, F. Meirer, A. Mehta, E. S. Uffelman, A. Hull, F. Vanmeert, J. Kieffer, M. Burghammer, K. Janssens, F. Sette, and J. Mass, Applied Physics A **121**, 967 (2015).

[6] G. Van der Snickt, K. Janssens, J. Dik, F. De Nolf, W. Vanmeert, J. Jaroszewicz, M. Cotte, G. Falkenberg, and L. Van der Loeff, Analytical Chemistry **84**, 10221 (2012).

[7] A. P. Davis and C. Huang, Water Research **25**, 1273 (1991).

[8] J. Paulus and U. Knuutinen, Applied Physics A **79**, 397 (2004).

[9] A. Romeo, D. Bätzner, H. Zogg, C. Vignali, and A. Tiwari, Solar Energy Materials and Solar Cells **67**, 311 (2001).

[10] A. L. Fahrenbruch and R. H. Bube, *Fundamentals of solar cells: photovoltaic solar energy conversion* (New York: Academic Press, 1983).

[11] T. Dzhafarov, M. Altunbas, A. I. Kopya, V. Novruzov, and E. Bacaksiz, Journal of Physics D: Applied Physics **32**, L125 (1999).

[12] X. Duan, Y. Huang, R. Agarwal, and C. Lieber, Nature **421**, 241 (2003).

[13] N. V. Hullavarad, S. S. Hullavarad, and P. C. Karulkar, Journal of Nanoscience and Nanotechnology **8**, 3272 (2008).

[14] A. Merkoçi, L. Humberto Marcolino-Junior, S. Marín, O. Fatibello-Filho, and S. Alegret, Nanotechnology **18**, 035502 (2007).

[15] B. A. Kulp, Phys. Rev. **125**, 1865 (1962).

[16] J. J. Ramsden and M. Gratzel, J. Chem. Soc., Faraday Trans. 1 **80**, 919 (1984).

[17] O. Cretu, C. Zhang, and D. Golberg, Applied Physics Letters **110**, 111904 (2017).

[18] M. Thoury, J. K. Delaney, E. R. de la Rie, M. Palmer, K. Morales, and K. Jay, Appl. Spectrosc. **65**, 939 (2011).
[19] A. Cesaratto, C. D'Andrea, A. Nevin, G. Valentini, F. Tassone, R. Alberti, T. Frizzi, and D. Comelli, Anal. Methods **6**, 130 (2014).
[20] F. Rosi, C. Grazia, F. Gabrieli, A. Romani, M. Paolantoni, R. Vivani, B. G. Brunetti, P. Colomban, and C. Miliani, Microchemical Journal **124**, 856 (2016).
[21] J. K. Delaney, J. G. Zeibel, M. Thoury, R. Littleton, M. Palmer, K. M. Morales, E. R. de la Rie, and A. Hoenigswald, Appl. Spectrosc. **64**, 584 (2010).
[22] P. Giannozzi *et al.*, Journal of Physics: Condensed Matter **21**, 395502 (2009).
[23] D. Vanderbilt, Phys. Rev. B **41**, 7892 (1990).
[24] J. P. Perdew, K. Burke, and M. Ernzerhof, Phys. Rev. Lett. **77**, 3865 (1996).
[25] L. A. Agapito, S. Curtarolo, and M. Buongiorno Nardelli, Phys. Rev. X **5**, 011006 (2015).
[26] L. Giacopetti and A. Satta, Journal of Physics: Conference Series **566**, 012021 (2015).
[27] L. Giacopetti and A. Satta, Microchemical Journal **126**, 214 (2016).
[28] L. Giacopetti and A. Satta, Microchemical Journal **137**, 502 (2018).
[29] P. Gopal, M. Fornari, S. Curtarolo, L. A. Agapito, L. S. I. Liyanage, and M. B. Nardelli, Phys. Rev. B **91**, 245202 (2015).
[30] F. Fabbri, M. Villani, A. Catellani, A. Calzolari, G. Cicero, D. Calestani, G. Calestani, A. Zappettini, B. Dierre, T. Sekiguchi, and G. Salviati, Sci. Rep. **4** (2014).
[31] J. P. Perdew and M. Levy, Phys. Rev. Lett. **51**, 1884 (1983).
[32] W. G. Aulbur, L. Jönsson, and J. W. Wilkins, Solid State Physics **54**, 1 (2000).
[33] J. Heyd, G. E. Scuseria, and M. Ernzerhof, The Journal of Chemical Physics **118**, 8207 (2003).
[34] C. Freysoldt, B. Grabowski, T. Hickel, J. Neugebauer, G. Kresse, A. Janotti, and C. G. Van de Walle, Rev. Mod. Phys. **86**, 253 (2014).
[35] H.-P. Komsa and A. Pasquarello, Phys. Rev. Lett. **110**, 095505 (2013).
[36] A. Varghese, P. Ghosh, and S. Datta, The Journal of Physical Chemistry C **118**, 21604 (2014).
[37] S. Lany and A. Zunger, Phys. Rev. B **78**, 235104 (2008).
[38] P. Dunning, *High Performance Pigments* (Wiley-VCH Verlag GmbH & Co. KGaA, 2003).
[39] A. Kobayashi, O. F. Sankey, and J. D. Dow, Phys. Rev. B **28**, 946 (1983).
[40] B. D. A. Levin, K. X. Nguyen, M. E. Holtz, M. B. Wiggins, M. G. Thomas, E. S. Tveit, J. L. Mass, R. Opila, T. Beebe, and D. A. Muller, Microscopy and Microanalysis **22**, 258 (2016).